The Alzheimer's Disease -Secretase Generates Higher 42:40 Ratios for -Amyloid Than for p3 Peptides

Siegel, Gabriele ; Gerber, Hermeto ; Koch, Philipp ; Bruestle, Oliver ; Fraering, Patrick C ; Rajendran, Lawrence

Abstract: Alzheimer's disease is characterized by intracerebral deposition of -amyloid (A). While A 40 is the most abundant form, neurotoxicity is mainly mediated by A 42. Sequential cleavage of amyloid precursor protein (APP) by - and -secretases gives rise to full-length A (A 1-x) and N-terminally truncated A ' (A 11-x) whereas cleavage by - and -secretases leads to the shorter p3 peptides (A 17-x). We uncovered significantly higher ratios of 42- versus 40-ending variants for A and A ' than for p3 secreted by mouse neurons and human induced pluripotent stem cell (iPSC)-derived neurons or produced in a cell-free -secretase assay with recombinant APP-CTFs. The 42:40 ratio was highest for A ', followed by A and then p3. Mass spectrometry analysis of APP intracellular domains revealed differential processing of APP-C83, APP-C89, and APP-C99 by -secretase already at the -cleavage stage. This mechanistic insight could aid in developing substrate-targeted modulators of APP-C99 processing to specifically lower the A 42:A 40 ratio without compromising -secretase function.

DOI: https://doi.org/10.1016/j.celrep.2017.05.034

Cell Reports

The Alzheimer's Disease γ-Secretase Generates Higher 42:40 Ratios for β-Amyloid Than for p3 Peptides

Graphical Abstract

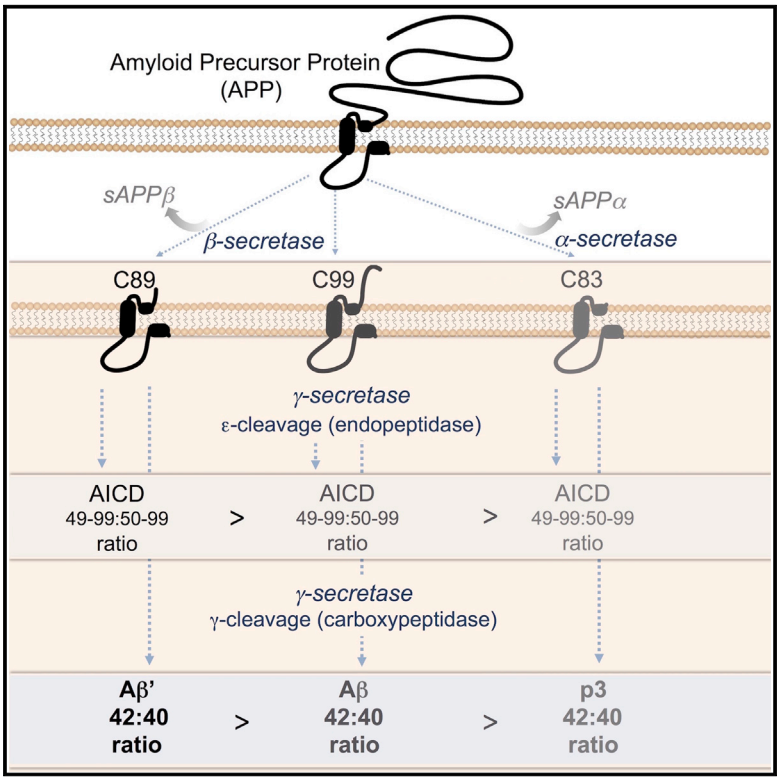

Highlights

- γ-Secretase produces Aβ and Aβ′ at a higher 42:40 ratio than p3 peptides
- The differential γ-cleavage of the three main APP-CTFs is substrate-driven
- AICD profiling shows that differential processing is initiated at the ε-cleavage stage

Authors

Gabriele Siegel, Hermeto Gerber, Philipp Koch, Oliver Bruestle, Patrick C. Fraering, Lawrence Rajendran

Correspondence

rajendran@bli.uzh.ch (L.R.), gabriele.siegel@irem.uzh.ch (G.S.)

In Brief

Siegel et al. find differences in the γ-secretase-mediated processing of the three major β-secretase- and α-secretase-cleaved C-terminal fragments of amyloid precursor protein (APP-C99, APP-C89, and APP-C83). Mouse and human neurons secrete significantly higher ratios of 42- versus 40-ending variants for Aβ and Aβ′ peptides than for p3 peptides.

Siegel et al., 2017, Cell Reports *19*, 1967–1976
June 6, 2017
http://dx.doi.org/10.1016/j.celrep.2017.05.034

CellPress

Cell Reports
Report

The Alzheimer's Disease γ-Secretase Generates Higher 42:40 Ratios for β-Amyloid Than for p3 Peptides

Gabriele Siegel,[1,*] Hermeto Gerber,[2,3,4] Philipp Koch,[5,6] Oliver Bruestle,[5,6] Patrick C. Fraering,[2,3] and Lawrence Rajendran[1,7,*]
[1]Systems and Cell Biology of Neurodegeneration, IREM, University of Zurich, Schlieren Campus, 8952 Schlieren, Switzerland
[2]Foundation Eclosion, 1228 Plan-les-Ouates & Campus Biotech Innovation Park, 1202 Geneva, Switzerland
[3]Brain Mind Institute and School of Life Sciences, Swiss Federal Institute of Technology (EPFL), 1015 Lausanne, Switzerland
[4]Department of Biology, University of Fribourg, 1700 Fribourg, Switzerland
[5]Institute of Reconstructive Neurobiology, University of Bonn Medical Faculty, 53127 Bonn, Germany
[6]LIFE & BRAIN GmbH, 53127 Bonn, Germany
[7]Lead Contact
*Correspondence: rajendran@bli.uzh.ch (L.R.), gabriele.siegel@irem.uzh.ch (G.S.)
http://dx.doi.org/10.1016/j.celrep.2017.05.034

SUMMARY

Alzheimer's disease is characterized by intracerebral deposition of β-amyloid (Aβ). While $Aβ_{40}$ is the most abundant form, neurotoxicity is mainly mediated by $Aβ_{42}$. Sequential cleavage of amyloid precursor protein (APP) by β- and γ-secretases gives rise to full-length Aβ ($Aβ_{1-x}$) and N-terminally truncated Aβ′ ($Aβ_{11-x}$) whereas cleavage by α- and γ-secretases leads to the shorter p3 peptides ($Aβ_{17-x}$). We uncovered significantly higher ratios of 42- versus 40-ending variants for Aβ and Aβ′ than for p3 secreted by mouse neurons and human induced pluripotent stem cell (iPSC)-derived neurons or produced in a cell-free γ-secretase assay with recombinant APP-CTFs. The 42:40 ratio was highest for Aβ′, followed by Aβ and then p3. Mass spectrometry analysis of APP intracellular domains revealed differential processing of APP-C83, APP-C89, and APP-C99 by γ-secretase already at the ε-cleavage stage. This mechanistic insight could aid in developing substrate-targeted modulators of APP-C99 processing to specifically lower the $Aβ_{42}$:$Aβ_{40}$ ratio without compromising γ-secretase function.

INTRODUCTION

Alzheimer's disease (AD), the most common neurodegenerative disease, is causally linked to the accumulation of misfolded β-amyloid (Aβ) peptides within the brain (Huang and Mucke, 2012; Selkoe, 2011). Aβ peptides, the length of which can vary from 37 to 43 amino acids (aa), are generated in the so-called amyloidogenic pathway through sequential proteolytic cleavage of the type-1 transmembrane amyloid precursor protein (APP) by two secretase entities, the aspartyl protease β-site APP cleaving enzyme 1 (BACE1, also termed β-secretase) and the tetrameric γ-secretase complex. β-secretase can cleave APP at two alternative sites, either at Asp_1 or at Glu_{11} of the Aβ sequence, leading to the generation of a 99 aa C-terminal fragment (CTF) (C99) or a 89 aa CTF (C89) that will then be further processed by γ-secretase to full-length $Aβ_{1-x}$ (Aβ) or the N-terminally truncated $Aβ_{11-x}$ (Aβ′), respectively (Thinakaran and Koo, 2008; Zhang et al., 2012). While Aβ′ appears to be the predominant species secreted by neurons and to contribute to the formation of insoluble aggregates in the brains of AD patients (Cai et al., 2001; Gouras et al., 1998; Liu et al., 2006), the two most abundant Aβ species found in senile plaques are $Aβ_{42}$ and $Aβ_{40}$. Production of Aβ and Aβ′ is precluded if APP is processed by α-secretase that cleaves within the Aβ sequence. The resulting 83 aa CTF (C83) is subsequently processed by γ-secretase, releasing the p3 peptide ($Aβ_{17-x}$). These ~3 kDa peptides are non-amyloidogenic but contribute to the formation of non-congophilic, diffuse plaques in the cerebellum of Down syndrome patients and different brain regions of AD patients (Gowing et al., 1994; Higgins et al., 1996; Lalowski et al., 1996). The pathological significance of this p3 accumulation is not yet understood.

The different C-terminal variants of Aβ, Aβ′, and p3 that are produced by γ-secretase arise from the carboxypeptidase-like trimming (γ-cleavage) of slightly longer membrane bound peptides that are generated through the initial endoproteolytic cleavage (ε-cleavage) of the respective APP CTFs. Whether the γ-secretase-mediated cleavage of APP-βCTFs and APP-αCTF is comparable with respect to the relative production of the different C-terminal variants of Aβ, Aβ′, and p3 is not known yet. The interpretation of data obtained from brain homogenates or cerebrospinal fluid (CSF) samples is difficult, since steady-state levels of the different Aβ, Aβ′, and p3 species in the brain are determined not only by their production but also by the continuous clearance through microglial phagocytosis and transport across the blood-brain barrier.

Here, we studied the relative levels of production of C-terminal variants of Aβ, Aβ′, and p3 in cellular systems where analyte levels are not significantly affected by microglial activity or sequestration into the blood stream (mouse primary neuronal

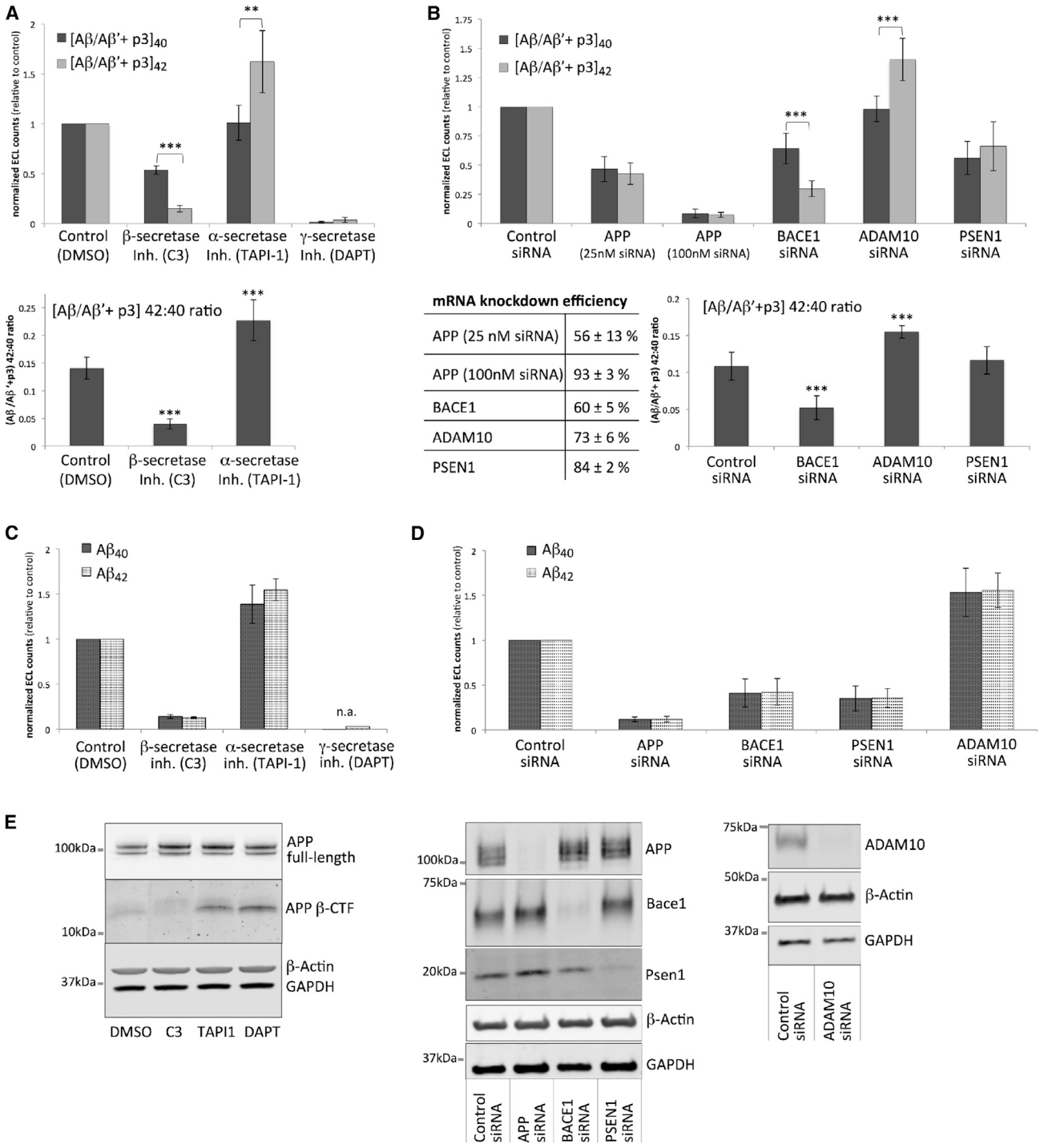

Figure 1. Interference with β-Secretase and with α-Secretase-Mediated APP-Processing Decreases and Increases, Respectively, the 42:40 Ratio of [Aβ/Aβ′+p3] Secreted by Mouse Primary Neurons

Wild-type mouse primary neurons were treated with β-secretase inhibitor (C3; 1 μM), α-secretase inhibitor (TAPI-1; 40 μM) or γ-secretase inhibitor (DAPT; 1 μM) or transfected with siRNAs targeting APP, BACE1, ADAM10, or PSEN1.

(A) Inhibitor-treated neurons. Top: relative $[Aβ/Aβ'+p3]_{40}$ and $[Aβ/Aβ'+p3]_{42}$ levels. Bottom: [Aβ/Aβ′+p3]42:40 ratio (n = 6 for C3 and TAPI-1; n = 4 for DAPT). Average ± SD. **p < 0.01; ***p < 0.001.

(B) siRNA-transfected neurons. Top: relative $[Aβ/Aβ'+p3]_{40}$ and $[Aβ/Aβ'+p3]_{42}$ levels. Table: mRNA knockdown efficiencies as analyzed by real-time PCR. Bottom: [Aβ/Aβ′+p3]42:40 ratio (n = 8 for BACE1 and PSEN1-siRNA; n = 5 for APP and ADAM10). Average ± SD. ***p < 0.001.

(legend continued on next page)

cultures and human induced pluripotent stem cell [iPSC]-derived neurons), as well as in a cell-free assay with purified γ-secretase. We made the surprising discovery that the 42:40 ratio is significantly different for all three peptide species (Aβ′ > Aβ > p3) as a consequence of differential γ-secretase-mediated ε-cleavage of the respective APP-CTFs. Our results could serve as a starting point for therapeutic deliberations that aim at altering specifically the Aβ production profile without changing physiological levels of other APP cleavage products nor interfering with the processing of other β-secretase and γ-secretase substrates.

RESULTS

For analysis of 40- and 42-ending C-terminal variants of p3 and Aβ/Aβ′ within the same assay, we used an electrochemiluminescence (ECL) multiplex immunoassay with C terminus-specific capture antibodies and a detection antibody that recognizes Aβ, Aβ′, and p3 peptides alike (4G8 monoclonal antibody [mAb]). In this way, we detected the total of all three peptides, discriminating only between the C termini. To uncover possible differences in the relative production of 40- and 42-ending variants of Aβ/Aβ′ versus p3 secreted by mouse primary neurons, we interfered with either the production of APP-βCTFs or APP-αCTF (in order to have only p3 or only Aβ/Aβ′ produced, respectively) and monitored the 42:40 ratios in comparison to the control condition where all analytes were present. Suppression of Aβ/Aβ′ production was achieved through incubation with β-secretase inhibitor and led to a strong reduction of the 42:40 ratio as the result of a more pronounced decrease of the $[Aβ/Aβ′+p3]_{42}$ signal compared to the $[Aβ/Aβ′+p3]_{40}$ signal (Figure 1A). Suppression of p3 production through α-secretase inhibition, on the other hand, increased the 42:40 ratio. For validation of our initial finding with a different method, we performed small interfering RNA (siRNA)-mediated knockdowns of either BACE1, the predominant β-secretase of APP (Cai et al., 2001; Vassar et al., 1999), or ADAM10, the predominant α-secretase of APP in neurons (Jorissen et al., 2010; Kuhn et al., 2010; Postina et al., 2004). Knockdown of BACE1 produced a pronounced decrease of the [Aβ/Aβ′+p3] 42:40 ratio whereas knockdown of ADAM10 increased the 42:40 ratio (Figure 1B), highly similar to the shift observed upon β-secretase and α-secretase inhibition. Importantly, simultaneous reduction of Aβ/Aβ′ and p3 by partial knockdown of APP or PSEN1, the catalytic subunit of the γ-secretase complex, did not alter the 42:40 ratio of the Aβ/Aβ′+p3 signal (Figure 1B), demonstrating that, under physiological conditions, a concentration shift between substrate (APP-CTF) and enzyme (γ-secretase) is not sufficient to reduce the 42:40 ratio, contrary to what has been observed in mutant APP transgenic cells by a previous study (Yin et al., 2007).

So far, our data show that the 42:40 ratio of the Aβ/Aβ′+p3 signal is reduced when the obtained signal is contributed mainly by p3 (= upon suppression of Aβ and Aβ′ production by interference with β-secretase) and increased when mainly Aβ and Aβ′ are produced (= upon suppression of p3 production by interference with α-secretase).

This suggests that either Aβ/Aβ′ are produced at a significantly higher 42:40 ratio than p3, or that interference with β-secretase or α-secretase indirectly affects γ-secretase-mediated processing of APP-CTFs. In order to dissect these two scenarios, we analyzed the 42:40 ratio of Aβ itself, which is expected to remain stable only in the first scenario. For specific detection of murine $Aβ_{40}$ and $Aβ_{42}$ we combined the ECL multiplex platform with a detection antibody (M3.2 mAb) that binds within aa 10–15 of murine Aβ, N-terminally of the APP α-secretase cleavage site.

When analyzing specifically Aβ, we no longer observed a shift in the 42:40 ratio (Figures 1C and 1D). Both $Aβ_{42}$ and $Aβ_{40}$ decreased in a highly comparable manner upon β-secretase inhibition or knockdown of BACE1 and increased upon α-secretase inhibition or ADAM10 knockdown. We therefore conclude that the observed 42:40 shift of the Aβ/Aβ′+p3 signal upon interference with β-secretase or α-secretase is indeed due to a higher 42:40 ratio for Aβ/Aβ′ peptides than for p3 peptides.

To test if our finding has a bearing in a more relevant context to humans, we validated our results in human iPSC-derived neurons. In agreement with our data from mouse primary neurons, we detected a disproportional decrease of $[Aβ/Aβ′+p3]_{42}$ compared to $[Aβ/Aβ′+p3]_{40}$ upon β-secretase inhibitor treatment, whereas α-secretase inhibition increased the 42:40 ratio (Figure 2A). The efficacy of β-secretase and α-secretase inhibition was monitored by ECL analysis of sAPPβ and sAPPα (Figure 2B). The ratio of $Aβ_{42}$ to $Aβ_{40}$ was again unchanged in both setups (Figure 2C).

Taken together, our results thus far show that both mouse and human neurons produce Aβ/Aβ′ peptides at a significantly higher 42:40 ratio than p3 peptides. This finding suggests that APP β-CTFs and α-CTFs are differentially processed by γ-secretase. What could cause this differential processing? Previous studies have described substrate specificity (cleavage of APP versus Notch) as well as differences in ε- and γ-processing (generation of different Aβ profiles) for specific γ-secretase complex compositions (Acx et al., 2014; Serneels et al., 2009). We considered the possibility that also APP β-CTFs and α-CTF might be processed by different γ-secretase complexes and that this specificity results in higher 42:40 ratios for Aβ/Aβ′ as compared to p3. A functional γ-secretase complex requires the assembly of four essential subunits: presenilin (PSEN), nicastrin (NCSTN), anterior pharynx-defective protein 1 (APH1), and presenilin enhancer γ-secretase subunit (PSENEN) (Edbauer et al., 2003). Both PSEN and APH1 show genetic heterogeneity, which permits the formation of at least four different γ-secretase complexes in human and six different complexes in mouse (Hébert et al., 2004). To test our hypothesis, we systematically interfered with the formation of the individual γ-secretase complexes by siRNA-mediated knockdown of PSEN homologs (PSEN1,

(C) Inhibitor-treated neurons. Relative $Aβ_{40}$ and $Aβ_{42}$ levels (n = 5 for C3; n = 7 for TAPI-1; n = 4 for DAPT). Average ± SD.
(D) siRNA-transfected neurons. Relative $Aβ_{40}$ and $Aβ_{42}$ levels (n = 5 for APP, BACE1, and PSEN1; n = 4 for ADAM10). Average ± SD.
(E) Western blot analysis of APP-full length and APP β-CTF upon β-, α-, and γ-secretase inhibitor treatment and validation of knockdown efficiency at protein level for APP, BACE1, PSEN1, and ADAM10.

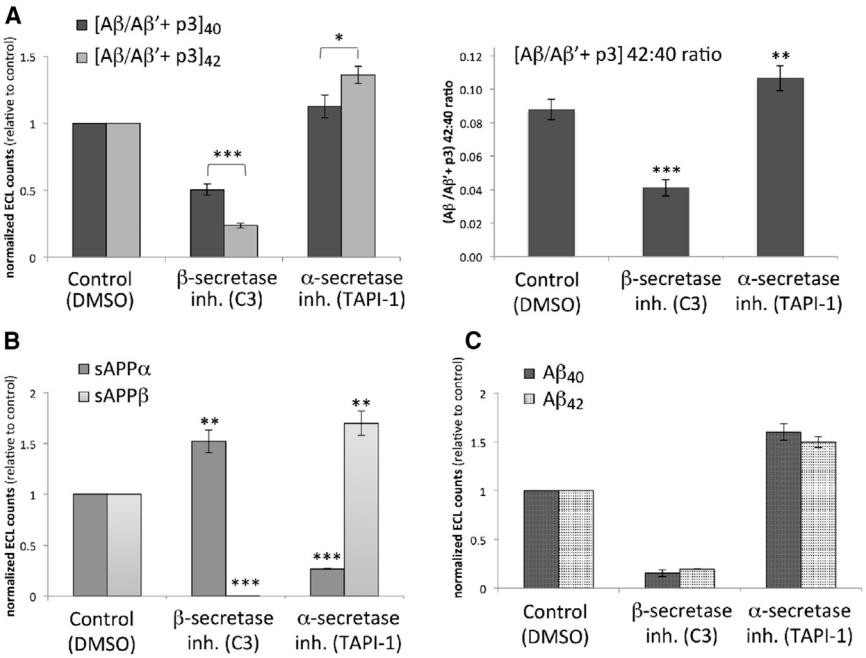

Figure 2. β-Secretase and α-Secretase Inhibition Decreases and Increases, Respectively, the 42:40 Ratio of [Aβ/Aβ′+p3] Secreted by Human iPSC-Derived Neurons

Human iPSC-derived neurons were treated with β-secretase inhibitor (C3; 1 μM) or α-secretase inhibitor (TAPI-1; 40 μM). Data are displayed as average ± SD of the averaged quadruplicate measurements for the two lines of human iPSC-derived neurons.

(A) Relative levels of $[Aβ/Aβ'+p3]_{40}$ and $[Aβ/Aβ'+p3]_{42}$ as analyzed by ECL assay (left) and the respective [Aβ/Aβ′+p3] 42:40 ratios (right). *$p < 0.05$; **$p < 0.01$; ***$p < 0.001$.

(B) Relative levels of sAPPβ and sAPPα as analyzed by ECL assay. **$p < 0.01$; ***$p < 0.001$.

(C) Relative levels of $Aβ_{40}$ and $Aβ_{42}$ as analyzed by ECL assay.

PSEN2) or APH1 homologs (APH1A, APH1B, APH1C) in mouse primary neurons and analyzed the 40:42 ratio of Aβ/Aβ′+p3 under basal conditions as well as upon β-secretase inhibitor treatment. Loss of PSEN or APH1 heterogeneity left the 40:42 ratio unchanged under basal conditions and did not affect the 42:40 ratio shift that occurs upon β-secretase inhibition (Figure 3A). These data suggest that the different 42:40 ratios of Aβ/Aβ′ versus p3 do not require the action of different γ-secretase complexes. While we are aware that silencing of the PSEN and APH1 homologs was incomplete, we believe that, with a knockdown efficiency of >60% at mRNA level and confirmed reduction at protein level for all detectable subunits (Figure 3B), individual γ-secretase complex subtypes have been sufficiently reduced to uncover possible effects.

Having shown that γ-secretase heterogeneity is not crucial for the differential processing of APP αCTF and βCTFs, we next studied whether the differential processing could be attributed to the substrates themselves. The two APP β-CTFs (C99 and C89) differ from APP α-CTF (C83) by an extended N terminus (16 aa and 10 aa, respectively) that might affect the positioning of the substrate toward the γ-secretase complex, thereby dictating the ε-cleavage site for initial proteolysis and consequently defining whether 40- or 42-C-terminal fragments are generated during the subsequent γ-cleavage steps (Olsson et al., 2014; Takami et al., 2009). Cleavage might also be modulated by the different pH of the subcellular compartments where γ-secretase meets APP α-CTF or β-CTFs. While α-secretase can cleave APP already at the cell surface, efficient β-secretase cleavage of APP requires the low pH of the endocytic compartment (Haass et al., 2012; Perez et al., 1999; Rajendran et al., 2006, 2008; Vassar et al., 1999). With active γ-secretase being present at both plasma membrane and endosomes (Kaether et al., 2006; Tarassishin et al., 2004), γ-secretase cleavage is likely to occur immediately after α- and β-cleavage in the respective subcellular compartments. To directly study the influence of substrate identity (APP-CTFs C83, C89, and C99) and pH environment on the 42:40 ratio of p3, Aβ′, and Aβ, we took advantage of a cell-free assay (Dimitrov et al., 2013) where recombinant human APP C83-His, C89-His, or C99-His substrates were incubated together with purified γ-secretase at four different pH (pH 5.5, pH 6.5, pH 7.5, and pH 8.5). Analysis of total APP intracellular domain (AICD) levels by western blot and analysis of Aβ, Aβ′, and p3 by ECL-assay showed highest γ-secretase activity at pH 6.5, in line with previous findings (Fraering et al., 2004; McLendon et al., 2000) (Figure 4A). Interestingly, the 42:40 ratio consistently decreased with lower pH for all three analytes (Aβ, Aβ′, and p3) (Figure 4A), suggesting that the low pH environment of the cellular endocytic compartment where Aβ and Aβ′ are produced does not contribute to the higher 42:40 ratio as compared to p3. The substrate itself (APP-CTF), however, had a strong influence on the 42:40 ratio of the respective cleavage products produced by γ-secretase. In a first experiment, where only APP C99 and C83 were studied, the 42:40 ratio of Aβ was found to be 2-fold higher than the 42:40 ratio of p3 peptides, and it was 1.4-fold higher in a second and third experiment, where all three APP CTFs were analyzed in parallel (Figure 4B). Very surprisingly, the 42:40 ratio of Aβ′ did not resemble either Aβ or p3, nor did it fall between these two, but it even exceeded the 42:40 ratio of Aβ (by 1.6-fold and 3.2-fold in experiment 2 and 3, respectively) (Figure 4B). To understand whether the different 42:40 ratios of Aβ, Aβ′, and p3 result from differential ε-cleavage or γ-cleavage of the respective APP-CTFs, we analyzed the AICD profiles generated from C83, C89, and C99 by mass spectrometry. Two different production lines have been postulated for the generation of $Aβ_{40}$ and $Aβ_{42}$ (Figure 4C), each of which is associated with the generation of one distinct AICD. The $AICD_{49–99}$ is produced in the $Aβ_{42}$ line and $AICD_{50–99}$ in the $Aβ_{40}$ line (Olsson et al., 2014; Takami et al., 2009). Mass spectrometry analysis showed that all three APP-CTFs gave rise to these two AICD species (Figure 4D).

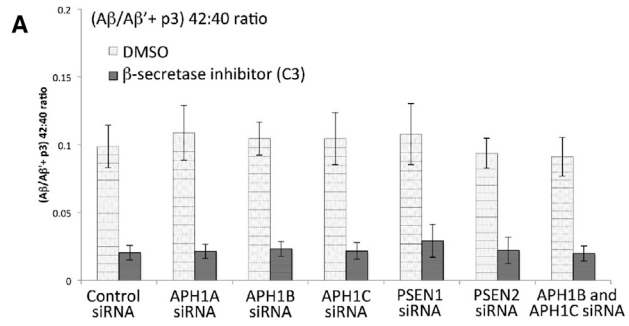

	mRNA knockdown efficiency	
	single knockdowns	APH1B/C double knockdown
APH1A	69 ± 9 %	
APH1B	68 ± 10 %	79 ± 5 %
APH1C	80 ± 6 %	83 ± 1 %
PSEN1	90 ± 0.5 %	
PSEN2	84 ± 4 %	

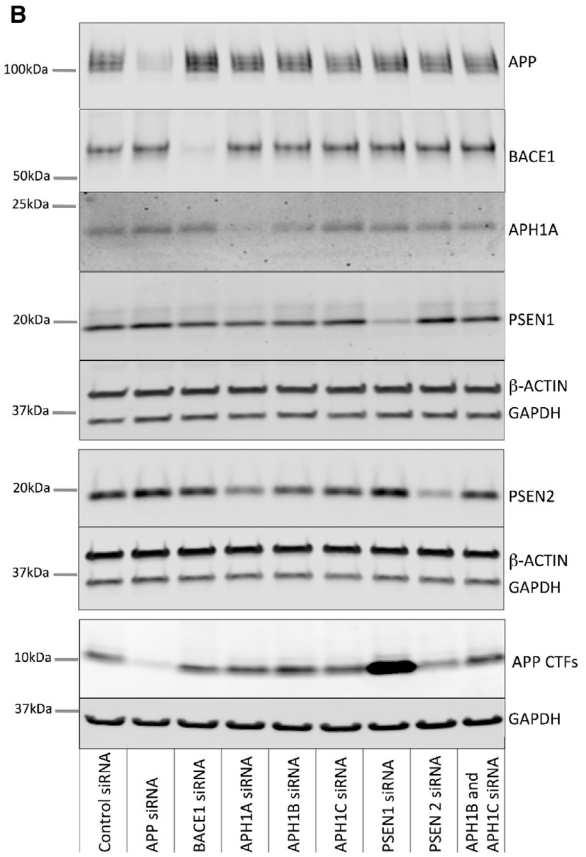

Figure 3. Limiting γ-Secretase Complex Heterogeneity by Knockdown of PSEN or APH1 Subunit Homologs Does Not Change the [Aβ/Aβ′+p3] 42:40 Ratio

Mouse primary neurons were transfected with siRNAs targeting APH1A, APH1B, APH1C, PSEN1, or PSEN2 (n = 3) and treated with DMSO or β-secretase inhibitor (C3; 1 μM).

(A) Relative [Aβ/Aβ′+p3] 42:40 ratios as analyzed by ECL. Average ± SD. Table: mRNA knockdown efficiencies as analyzed by real-time PCR.

(B) Western blot analysis of protein levels for the different knockdown conditions. APH1B/C signal was not detectable (see Figure S2).

However, the relative peak intensity of both AICDs differed significantly between the different substrates. The highest ratio of $AICD_{49–99}$:$AICD_{50–99}$ was produced from APP C89, followed by C99 and then by C83 (Figure 4D). The $AICD_{49–99}$:$AICD_{50–99}$ ratios produced from C89, C99, and C83 thus follow the same order as the 42:40 ratios for Aβ′, Aβ, and p3. This suggests that the different 42:40 ratios are the consequence of differential ε-cleavage of the three APP-CTFs by γ-secretase.

It is intriguing that the 42:40 ratio of Aβ′ does not fall in between Aβ and p3 and that it is even higher than for Aβ. We wanted to validate this observation in a cellular setting using a previously characterized pertinent mutation in APP. The Leuven mutation (APP^{695}_{E607K}) affects the alternative β-secretase cleavage site at position +11 and shifts β-secretase cleavage to the +1 site (Zhou et al., 2011). This shift results in more full-length Aβ at the expense of Aβ′ and would allow us to detect differences in the 42:40 ratios between both peptides. As a cellular system, we used HEK293 cells that stably express BACE1 (HEK-BACE1), which show dominant β-secretase activity (Figure 5A) and negligible contribution of endogenous APP-derived products to the obtained Aβ/Aβ′+p3 signal (the low reads from GFP-transfected cells were insensitive to γ-secretase inhibition and therefore considered as unspecific background; data not shown). HEK-BACE1 cells were transfected with plasmids expressing either wild-type human APP^{695}, the Leuven mutation APP^{695}_{E607K} or one of two other +11 site mutations (APP^{695}_{E607A} and $APP^{695}_{\Delta 607}$). Western blot analysis of APP β-CTFs under γ-secretase inhibitor treatment showed an increased APP C99:C89 ratio (a shift from the +11 to the +1 site) for APP^{695}_{E607K} and for $APP^{695}_{\Delta 607}$ (Figure 5B). At the same time, the 42:40 ratio of the Aβ/Aβ′+p3 signal was significantly decreased for these two mutations as compared to $APP^{695}_{wild\text{-}type}$ (Figure 5C). This difference was abolished by β-secretase inhibitor treatment and unaffected by α-secretase inhibitor treatment, demonstrating that it is produced solely by β-secretase cleavage-derived products (Aβ+Aβ′). Because both the APP^{695}_{E607K} and the $APP^{695}_{\Delta 607}$ mutation increase the C99:C83 ratio and accordingly the Aβ:Aβ′ ratio, the lower 42:40 ratio of the obtained Aβ+Aβ′ signal can thus be attributed to a lower 42:40 ratio of full-length Aβ as compared to Aβ′, which confirms our results from the cell free γ-secretase assay.

In summary, our results describe a differential processing of the three main APP-CTFs (C99, C89, and C83) by γ-secretase. Differential processing is initiated at the level of ε-cleavage, leading to different $AICD_{49–99}$:$AICD_{50–99}$ ratios produced from C99, C89, and C83, and continues during γ-cleavage that results in significantly different 42:40 ratios for Aβ, Aβ′, and p3 peptides.

DISCUSSION

The three major APP-CTFs (C99, C89, and C83) differ only in the length of their ectodomains and in their free N termini. γ-Secretase cleavage takes place within the hydrophobic environment of the membrane lipid bilayer that is not accessible to the hydrophilic N terminus. This raises the question as to how the different ectodomains modulate ε-/γ-cleavage of the respective APP-CTFs. Substrate recruitment by γ-secretase was initially proposed to require interaction of the substrate's free N terminus

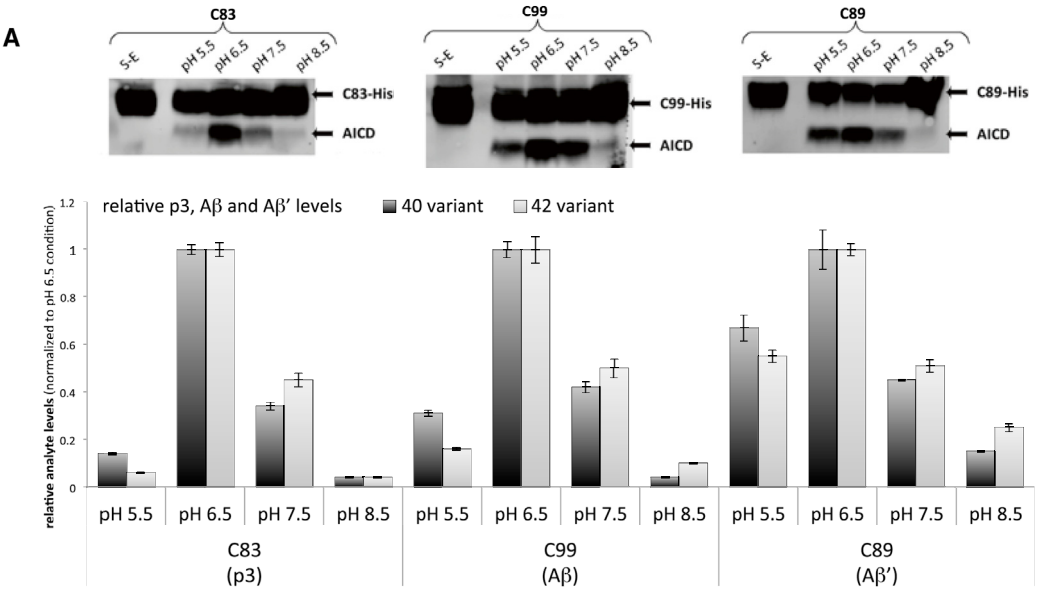

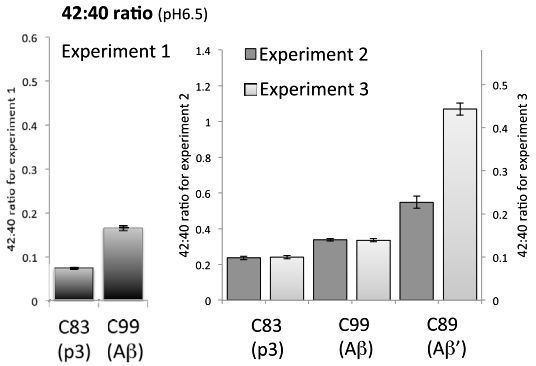

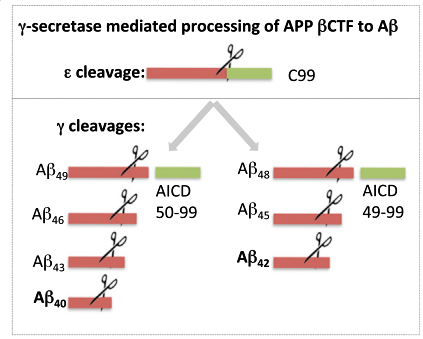

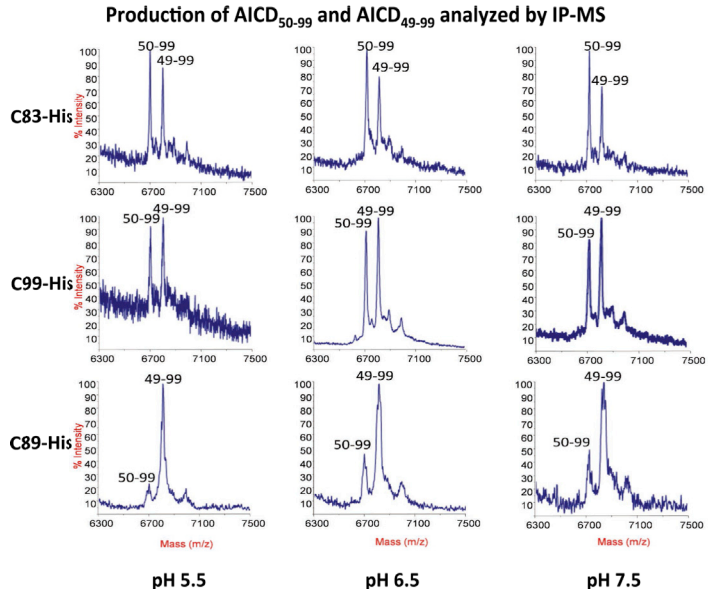

ratio
AICD 49-99 : AICD 50-99

C83	0.84	0.81	0.74
C99	1.08	1.15	1.16
C89	4.12	2.20	2.02
	pH 5.5	pH 6.5	pH 7.5

(legend on next page)

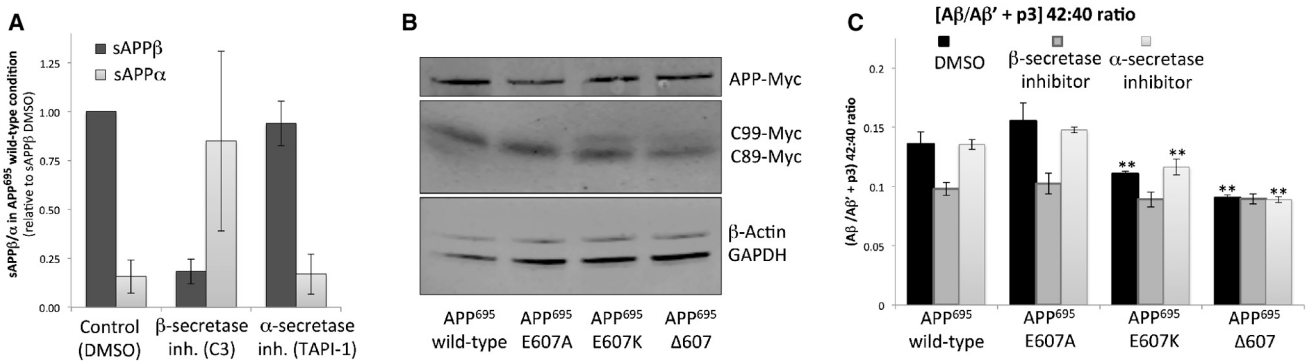

Figure 5. A Shift from Aβ′ to Aβ Production Is Associated with Lower 42:40 Ratios

HEK-BACE1 cells were transfected with different APP-expressing constructs and treated with DMSO, β-secretase inhibitor (C3; 2 μM), or α-secretase inhibitor (TAPI-1; 40 μM).

(A) ECL analysis of relative sAPPα and sAPPβ levels (n = 3). Average ± SD.

(B) Western blot analysis of APP full-length and APP-CTFs in DAPT-treated cells.

(C) ECL-analysis of 42:40 ratios of [Aβ/Aβ′+p3]. n = 3; average ± SD. **p < 0.01.

with the nicastrin ectodomain (Shah et al., 2005). However, this model was challenged by independent functional studies that could not establish a role for the substrate's N terminus, or the substrate's ectodomain generally, in the recruitment by γ-secretase (Bolduc et al., 2016; Chávez-Gutiérrez et al., 2008). Instead, nicastrin's bulky ectodomain was found to play a role in passive substrate sorting by sterically blocking the access of substrates that have not yet undergone shedding by α- or β-secretase (Bolduc et al., 2016). Interestingly, even for shed substrates, cleavage efficiency appears to decline with increasing ectodomain length, making APP C99 a less favored γ-secretase substrate than APP C83 (Funamoto et al., 2013). We observed, however, no correlation of that type between the APP-CTF ectodomain length and the 49–99:50–99 ratios of AICDs or the 42:40 ratios of Aβ, Aβ′, and p3 peptides. APP-C89, which has an ectodomain length that ranges between APP-C83 and APP-C99, produced the highest 49–99:50–99 and 42:40 ratios of all three APP-CTFs. The APP-CTF ectodomain length per se is thus not able to modulate γ-secretase-mediated ε- or γ-cleavage into a specific direction.

The APP-CTF ectodomain features a so-called APP substrate inhibitory domain (ASID) that comprises a stretch of five hydrophobic residues (LVFFA; corresponding to Aβ 17–21), which interact with PSEN and negatively regulate γ-secretase activity in an allosteric manner (Fukumori and Steiner, 2016; Tian et al., 2010). Interestingly, deletion and mutations of this region disproportionally affect $Aβ_{40}$ and $Aβ_{42}$ production in both cell-based and in vitro assays (De Jonghe et al., 1998; Tang et al., 2014; Tian et al., 2010). Structural analysis of APP-C99 revealed that the LVFFA motif forms the central stretch of a surface-associated α-helix that is flanked by a short juxtamembrane luminal loop that connects to the transmembrane domain (TMD) and by a disordered 16 aa stretch on the N-terminal side (Beel et al., 2008; Nadezhdin et al., 2011; Pester et al., 2013). It is conceivable that the proposed membrane-embedding of the ASID helix (Beel et al., 2008) and its mobility within the bilayer differ slightly between the three APP-CTFs as a result of the different numbers of residues located N-terminal of the helix and their intermolecular interactions with e.g., the nicastrin ectodomain or lipid headgroups of the membrane. This could affect the interaction of ASID with PSEN and/or modulate the accessibility and helical stability of the ε-cleavage sites Thr48 and Leu49 in APP-TMD through direct or allosteric effects as seen for familial AD mutations (Chen et al., 2014) and translate into differential ε-/γ-cleavage. In APP-C83, the 16 aa N-terminal truncation as compared to APP-C99 moves the N terminus to the first residue of the LVFFA domain thereby rendering the otherwise hydrophobic leucine positively charged and directly affecting the ASID motif. In APP-C89, the 10 aa N-terminal truncation removes most of the residues that have been identified by photoaffinity mapping to be the primary contact sites with nicastrin (Fukumori and Steiner, 2016). The mobility of the ASID harboring ectodomain of APP-C89 is therefore expected to be much less affected by nicastrin than the ectodomain of APP-C99.

Our pH profiling analysis suggests that, in addition to substrate identity, the pH of the subcellular compartment where γ-secretase cleavage takes place can additionally modulate the interaction between APP-CTFs and γ-secretase. This

Figure 4. Differential ε-Cleavage of APP C83, C99, and C89 Results in Different 42:40 Ratios for p3, Aβ, and Aβ′

Recombinant APP C83-His, APP C99-His, or APP C89-His were cleaved by purified γ-secretase at different pH.

(A) Top: Western blot analysis of AICD-His. Bottom: ECL-analysis of relative p3, Aβ, and Aβ′ levels. Average ± SD of triplicate measurements.

(B) ECL analysis of 42:40 ratios of p3, Aβ, and Aβ′ (pH 6.5). Average ± SD of triplicate measurements.

(C) Postulated model for γ-secretase-mediated processing of APP C99 where Aβ42 and Aβ40 are generated in two different production lines.

(D) Immunoprecipitation (IP) MALDI-TOF mass spectrometry analysis of AICD species generated from C83-His, C99-His, and C89-His. Table: $AICD_{49–99}$: $AICD_{50–99}$ ratios as estimated from peak intensities.

modulation would, however, not contribute to the higher 42:40 ratios observed for Aβ and Aβ′ because the 42:40 production ratios were found to decrease in low pH conditions, representative of the endocytic compartment where APP-βCTFs are produced. Our data point to the substrate itself as the major determinant for the differential processing of the three APP-CTFs. Considering the high neurotoxicity that is caused by $A\beta_{42}$ as compared to $A\beta_{40}$, one wonders whether the newly acquired knowledge about the impact of the different APP-CTF ectodomains on γ-secretase cleavage can be exploited to modulate the processing of APP-C99 so as to specifically lower the production of toxic $A\beta_{42}$. By physically shielding the N-terminal region of APP-C99 it should be possible to confine the interaction with γ-secretase to APP-C83 residues. Such masking might render γ-secretase processing of APP-C99 more "C83-like" and reduce the resulting Aβ 42:40 ratio. Our finding that the 42:40 ratio of Aβ′ that is produced from APP C89 exceeds the 42:40 ratio of Aβ suggests that a successful modulation into the desired direction would require masking of the entire 16 N-terminal amino acids of APP C99 in order to avoid "C89-like" processing. However, because the actual outcome of such manipulations is hardly foreseeable, especially with respect to the previously discussed intermolecular interactions of the APP-CTF ectodomain with nicastrin and/or the membrane surface and its impact on the ASID helix, a systematic experimental testing is needed to identify the optimal approach. Modulation of APP-βCTF processing by targeting the substrate itself would have a significant advantage over classical strategies that aim at reducing Aβ production through inhibition of β-secretase or γ-secretase, that is the unperturbed processing of all physiological β-secretase and γ-secretase substrates. Importantly, this includes APP, which is the precursor not only for Aβ but also for several other cleavage products (e.g., p3, sAPPα, sAPPβ, and AICD) that can affect physiological functions on their part (Chasseigneaux and Allinquant, 2012; Nhan et al., 2015). An intervention strategy that would allow us to modulate specifically the Aβ production profile without compromising the processing of other β-secretase and γ-secretase substrates nor altering physiological levels of other APP cleavage products would therefore be highly desirable in order to minimize the risk of potential negative side effects.

EXPERIMENTAL PROCEDURES

Mouse Primary Neuronal Cultures

Mixed cortical/hippocampal primary neuronal cultures were prepared from E16 ICR (CD-1) outbred mice (Harlan Laboratories). All animal experiments were done according to the guidelines of and approved by the veterinary office of the Canton of Zürich, Switzerland. For details see the Supplemental Experimental Procedures.

Human iPSC-Derived Neurons

iPSCs from two healthy male donors (33 and 34 years old) have been generated previously (Mertens et al., 2013). For details on neuronal differentiation and culture conditions see the Supplemental Experimental Procedures.

siRNA Transfection

4DIV primary neurons were transfected with 100 nM of siRNA (stealth siRNA, Life Technologies) using Lipofectamine RNAiMax (Life Technologies) as transfection reagent. For details see the Supplemental Experimental Procedures.

Inhibitor Treatment

The following inhibitors were used: α-secretase inhibitor TAPI-1, β-secretase inhibitor IV, and γ-secretase inhibitor DAPT (all from Calbiochem, Merck Millipore). 7 days in vitro (DIV) primary neurons and HEK-BACE1 cells were treated for 24 hr (72 hr post-transfection), human iPSC-derived neurons for 20 hr (following a preincubation for 16 hr).

Electrochemiluminescence Assay

Twenty-four hour conditioned medium of 8DIV mouse primary neurons or HEK-BACE1 cells (72 hr post-transfection) or 20 hr conditioned medium of human iPSC-derived neurons was used for analysis. Mouse or human $[A\beta/A\beta'+p3]_{40}$ and $[A\beta/A\beta'+p3]_{42}$ were analyzed with the Aβ-Panel-1 Kit (4G8) (Meso-Scale-Discovery). Murine $A\beta_{40}$ and $A\beta_{42}$ were analyzed with the Aβ-Panel-1 Kit assay plate (Meso-Scale-Discovery) together with SULFO-TAG anti mouse/rat-Aβ (M3.2 mAb) antibody. sAPPα and sAPPβ were analyzed with the sAPPα/sAPPβ multiplex assay (Meso-Scale-Discovery). Standard curves are depicted in Figure S1. For details see the Supplemental Experimental Procedures.

γ-Secretase Activity Assay

γ-Secretase assays using recombinant human APP C99-His, C89-His, and C83-His were performed as previously reported (Cacquevel et al., 2008; Dimitrov et al., 2013; Wu et al., 2010). For details see the Supplemental Experimental Procedures.

Statistical Analysis

Data are represented as average ± SD. All p values were determined using two-tailed Student's t test. Paired testing was applied for comparison of different relative analyte levels within a given experimental condition. Unpaired testing was performed for comparison to the control condition.

Additional information on materials and methods can be found in Supplemental Experimental Procedures.

SUPPLEMENTAL INFORMATION

Supplemental Information includes Supplemental Experimental Procedures and two figures and can be found with this article online at http://dx.doi.org/10.1016/j.celrep.2017.05.034.

AUTHOR CONTRIBUTIONS

G.S., P.C.F., and L.R. designed the study. G.S. performed experiments in primary neurons and HEK-BACE1 cells. H.G. performed γ-secretase assay experiments and mass spectrometry analyses. P.K. performed human iPSC experiments. G.S. and L.R. wrote the paper. All authors participated in designing the experiments, in data analysis, and in the editing of the paper.

ACKNOWLEDGMENTS

We thank Prof. Bart De Strooper for providing APH1A and APH1B/C antibodies and Dr. Uwe Konietzko for providing the $APP^{695}{}_{wildtype}$ plasmid. We thank Prof. Dieter Langosch and Dr. Christina Scharnagl for their comments on the manuscript. L.R. was supported by the Swiss National Science Foundation (SNF) (Sinergia and Core Interdisciplinary grants, 31003A_146471 / CR33I3_153039 / IZ73Z0_152496), the Velux Foundation (Proj. 870), the Novartis Foundation, the Bangerter Stiftung, the Baugarten Stiftung, and the Synapsis Foundation. H.G. and P.C.F. were supported by the SNF (grant 31003A_152677/1) and the Strauss Foundation. P.K. and O.B. were supported by the German Federal Ministry for Education and Research (BMBF: BioPharma-NeuroAllianz grants 1615608A and 1615608B). G.S. was supported by an EMBO long-term fellowship (ALTF 668-2011) and the University of Zurich's Forschungskredit (K-82033-02-01).

Received: January 7, 2016
Revised: March 12, 2017
Accepted: May 9, 2017
Published: June 6, 2017

REFERENCES

Acx, H., Chávez-Gutiérrez, L., Serneels, L., Lismont, S., Benurwar, M., Elad, N., and De Strooper, B. (2014). Signature amyloid β profiles are produced by different γ-secretase complexes. J. Biol. Chem. *289*, 4346–4355.

Beel, A.J., Mobley, C.K., Kim, H.J., Tian, F., Hadziselimovic, A., Jap, B., Prestegard, J.H., and Sanders, C.R. (2008). Structural studies of the transmembrane C-terminal domain of the amyloid precursor protein (APP): does APP function as a cholesterol sensor? Biochemistry *47*, 9428–9446.

Bolduc, D.M., Montagna, D.R., Gu, Y., Selkoe, D.J., and Wolfe, M.S. (2016). Nicastrin functions to sterically hinder γ-secretase-substrate interactions driven by substrate transmembrane domain. Proc. Natl. Acad. Sci. USA *113*, E509–E518.

Cacquevel, M., Aeschbach, L., Osenkowski, P., Li, D., Ye, W., Wolfe, M.S., Li, H., Selkoe, D.J., and Fraering, P.C. (2008). Rapid purification of active gamma-secretase, an intramembrane protease implicated in Alzheimer's disease. J. Neurochem. *104*, 210–220.

Cai, H., Wang, Y., McCarthy, D., Wen, H., Borchelt, D.R., Price, D.L., and Wong, P.C. (2001). BACE1 is the major beta-secretase for generation of Abeta peptides by neurons. Nat. Neurosci. *4*, 233–234.

Chasseigneaux, S., and Allinquant, B. (2012). Functions of Aβ, sAPPα and sAPPβ : similarities and differences. J. Neurochem. *120* (*Suppl 1*), 99–108.

Chávez-Gutiérrez, L., Tolia, A., Maes, E., Li, T., Wong, P.C., and de Strooper, B. (2008). Glu(332) in the Nicastrin ectodomain is essential for gamma-secretase complex maturation but not for its activity. J. Biol. Chem. *283*, 20096–20105.

Chen, W., Gamache, E., Rosenman, D.J., Xie, J., Lopez, M.M., Li, Y.M., and Wang, C. (2014). Familial Alzheimer's mutations within APPTM increase Aβ42 production by enhancing accessibility of ε-cleavage site. Nat. Commun. *5*, 3037.

De Jonghe, C., Zehr, C., Yager, D., Prada, C.M., Younkin, S., Hendriks, L., Van Broeckhoven, C., and Eckman, C.B. (1998). Flemish and Dutch mutations in amyloid beta precursor protein have different effects on amyloid beta secretion. Neurobiol. Dis. *5*, 281–286.

Dimitrov, M., Alattia, J.R., Lemmin, T., Lehal, R., Fligier, A., Houacine, J., Hussain, I., Radtke, F., Dal Peraro, M., Beher, D., and Fraering, P.C. (2013). Alzheimer's disease mutations in APP but not γ-secretase modulators affect epsilon-cleavage-dependent AICD production. Nat. Commun. *4*, 2246.

Edbauer, D., Winkler, E., Regula, J.T., Pesold, B., Steiner, H., and Haass, C. (2003). Reconstitution of gamma-secretase activity. Nat. Cell Biol. *5*, 486–488.

Fraering, P.C., Ye, W., Strub, J.M., Dolios, G., LaVoie, M.J., Ostaszewski, B.L., van Dorsselaer, A., Wang, R., Selkoe, D.J., and Wolfe, M.S. (2004). Purification and characterization of the human gamma-secretase complex. Biochemistry *43*, 9774–9789.

Fukumori, A., and Steiner, H. (2016). Substrate recruitment of γ-secretase and mechanism of clinical presenilin mutations revealed by photoaffinity mapping. EMBO J. *35*, 1628–1643.

Funamoto, S., Sasaki, T., Ishihara, S., Nobuhara, M., Nakano, M., Watanabe-Takahashi, M., Saito, T., Kakuda, N., Miyasaka, T., Nishikawa, K., et al. (2013). Substrate ectodomain is critical for substrate preference and inhibition of γ-secretase. Nat. Commun. *4*, 2529.

Gouras, G.K., Xu, H., Jovanovic, J.N., Buxbaum, J.D., Wang, R., Greengard, P., Relkin, N.R., and Gandy, S. (1998). Generation and regulation of beta-amyloid peptide variants by neurons. J. Neurochem. *71*, 1920–1925.

Gowing, E., Roher, A.E., Woods, A.S., Cotter, R.J., Chaney, M., Little, S.P., and Ball, M.J. (1994). Chemical characterization of A beta 17-42 peptide, a component of diffuse amyloid deposits of Alzheimer disease. J. Biol. Chem. *269*, 10987–10990.

Haass, C., Kaether, C., Thinakaran, G., and Sisodia, S. (2012). Trafficking and proteolytic processing of APP. Cold Spring Harb. Perspect. Med. *2*, a006270.

Hébert, S.S., Serneels, L., Dejaegere, T., Horré, K., Dabrowski, M., Baert, V., Annaert, W., Hartmann, D., and De Strooper, B. (2004). Coordinated and widespread expression of gamma-secretase in vivo: evidence for size and molecular heterogeneity. Neurobiol. Dis. *17*, 260–272.

Higgins, L.S., Murphy, G.M., Jr., Forno, L.S., Catalano, R., and Cordell, B. (1996). P3 beta-amyloid peptide has a unique and potentially pathogenic immunohistochemical profile in Alzheimer's disease brain. Am. J. Pathol. *149*, 585–596.

Huang, Y., and Mucke, L. (2012). Alzheimer mechanisms and therapeutic strategies. Cell *148*, 1204–1222.

Jorissen, E., Prox, J., Bernreuther, C., Weber, S., Schwanbeck, R., Serneels, L., Snellinx, A., Craessaerts, K., Thathiah, A., Tesseur, I., et al. (2010). The disintegrin/metalloproteinase ADAM10 is essential for the establishment of the brain cortex. J. Neurosci. *30*, 4833–4844.

Kaether, C., Schmitt, S., Willem, M., and Haass, C. (2006). Amyloid precursor protein and Notch intracellular domains are generated after transport of their precursors to the cell surface. Traffic *7*, 408–415.

Kuhn, P.H., Wang, H., Dislich, B., Colombo, A., Zeitschel, U., Ellwart, J.W., Kremmer, E., Rossner, S., and Lichtenthaler, S.F. (2010). ADAM10 is the physiologically relevant, constitutive alpha-secretase of the amyloid precursor protein in primary neurons. EMBO J. *29*, 3020–3032.

Lalowski, M., Golabek, A., Lemere, C.A., Selkoe, D.J., Wisniewski, H.M., Beavis, R.C., Frangione, B., and Wisniewski, T. (1996). The "nonamyloidogenic" p3 fragment (amyloid beta17-42) is a major constituent of Down's syndrome cerebellar preamyloid. J. Biol. Chem. *271*, 33623–33631.

Liu, K., Solano, I., Mann, D., Lemere, C., Mercken, M., Trojanowski, J.Q., and Lee, V.M. (2006). Characterization of Abeta11-40/42 peptide deposition in Alzheimer's disease and young Down's syndrome brains: implication of N-terminally truncated Abeta species in the pathogenesis of Alzheimer's disease. Acta Neuropathol. *112*, 163–174.

McLendon, C., Xin, T., Ziani-Cherif, C., Murphy, M.P., Findlay, K.A., Lewis, P.A., Pinnix, I., Sambamurti, K., Wang, R., Fauq, A., and Golde, T.E. (2000). Cell-free assays for gamma-secretase activity. FASEB J. *14*, 2383–2386.

Mertens, J., Stüber, K., Wunderlich, P., Ladewig, J., Kesavan, J.C., Vandenberghe, R., Vandenbulcke, M., van Damme, P., Walter, J., Brüstle, O., and Koch, P. (2013). APP processing in human pluripotent stem cell-derived neurons is resistant to NSAID-based γ-secretase modulation. Stem Cell Reports *1*, 491–498.

Nadezhdin, K.D., Bocharova, O.V., Bocharov, E.V., and Arseniev, A.S. (2011). Structural and dynamic study of the transmembrane domain of the amyloid precursor protein. Acta Naturae *3*, 69–76.

Nhan, H.S., Chiang, K., and Koo, E.H. (2015). The multifaceted nature of amyloid precursor protein and its proteolytic fragments: friends and foes. Acta Neuropathol. *129*, 1–19.

Olsson, F., Schmidt, S., Althoff, V., Munter, L.M., Jin, S., Rosqvist, S., Lendahl, U., Multhaup, G., and Lundkvist, J. (2014). Characterization of intermediate steps in amyloid beta (Aβ) production under near-native conditions. J. Biol. Chem. *289*, 1540–1550.

Perez, R.G., Soriano, S., Hayes, J.D., Ostaszewski, B., Xia, W., Selkoe, D.J., Chen, X., Stokin, G.B., and Koo, E.H. (1999). Mutagenesis identifies new signals for beta-amyloid precursor protein endocytosis, turnover, and the generation of secreted fragments, including Abeta42. J. Biol. Chem. *274*, 18851–18856.

Pester, O., Barrett, P.J., Hornburg, D., Hornburg, P., Pröbstle, R., Widmaier, S., Kutzner, C., Dürrbaum, M., Kapurniotu, A., Sanders, C.R., et al. (2013). The backbone dynamics of the amyloid precursor protein transmembrane helix provides a rationale for the sequential cleavage mechanism of γ-secretase. J. Am. Chem. Soc. *135*, 1317–1329.

Postina, R., Schroeder, A., Dewachter, I., Bohl, J., Schmitt, U., Kojro, E., Prinzen, C., Endres, K., Hiemke, C., Blessing, M., et al. (2004). A disintegrin-metalloproteinase prevents amyloid plaque formation and hippocampal defects in an Alzheimer disease mouse model. J. Clin. Invest. *113*, 1456–1464.

Rajendran, L., Honsho, M., Zahn, T.R., Keller, P., Geiger, K.D., Verkade, P., and Simons, K. (2006). Alzheimer's disease beta-amyloid peptides are released in association with exosomes. Proc. Natl. Acad. Sci. USA *103*, 11172–11177.

Rajendran, L., Schneider, A., Schlechtingen, G., Weidlich, S., Ries, J., Braxmeier, T., Schwille, P., Schulz, J.B., Schroeder, C., Simons, M., et al. (2008). Efficient inhibition of the Alzheimer's disease beta-secretase by membrane targeting. Science *320*, 520–523.

Selkoe, D.J. (2011). Alzheimer's disease. Cold Spring Harb. Perspect. Biol. *3*, a004457.

Serneels, L., Van Biervliet, J., Craessaerts, K., Dejaegere, T., Horré, K., Van Houtvin, T., Esselmann, H., Paul, S., Schäfer, M.K., Berezovska, O., et al. (2009). gamma-Secretase heterogeneity in the Aph1 subunit: relevance for Alzheimer's disease. Science *324*, 639–642.

Shah, S., Lee, S.F., Tabuchi, K., Hao, Y.H., Yu, C., LaPlant, Q., Ball, H., Dann, C.E., 3rd, Südhof, T., and Yu, G. (2005). Nicastrin functions as a gamma-secretase-substrate receptor. Cell *122*, 435–447.

Takami, M., Nagashima, Y., Sano, Y., Ishihara, S., Morishima-Kawashima, M., Funamoto, S., and Ihara, Y. (2009). gamma-Secretase: successive tripeptide and tetrapeptide release from the transmembrane domain of beta-carboxyl terminal fragment. J. Neurosci. *29*, 13042–13052.

Tang, T.C., Hu, Y., Kienlen-Campard, P., El Haylani, L., Decock, M., Van Hees, J., Fu, Z., Octave, J.N., Constantinescu, S.N., and Smith, S.O. (2014). Conformational changes induced by the A21G Flemish mutation in the amyloid precursor protein lead to increased Aβ production. Structure *22*, 387–396.

Tarassishin, L., Yin, Y.I., Bassit, B., and Li, Y.M. (2004). Processing of Notch and amyloid precursor protein by gamma-secretase is spatially distinct. Proc. Natl. Acad. Sci. USA *101*, 17050–17055.

Thinakaran, G., and Koo, E.H. (2008). Amyloid precursor protein trafficking, processing, and function. J. Biol. Chem. *283*, 29615–29619.

Tian, Y., Bassit, B., Chau, D., and Li, Y.M. (2010). An APP inhibitory domain containing the Flemish mutation residue modulates gamma-secretase activity for Abeta production. Nat. Struct. Mol. Biol. *17*, 151–158.

Vassar, R., Bennett, B.D., Babu-Khan, S., Kahn, S., Mendiaz, E.A., Denis, P., Teplow, D.B., Ross, S., Amarante, P., Loeloff, R., et al. (1999). Beta-secretase cleavage of Alzheimer's amyloid precursor protein by the transmembrane aspartic protease BACE. Science *286*, 735–741.

Wu, F., Schweizer, C., Rudinskiy, N., Taylor, D.M., Kazantsev, A., Luthi-Carter, R., and Fraering, P.C. (2010). Novel gamma-secretase inhibitors uncover a common nucleotide-binding site in JAK3, SIRT2, and PS1. FASEB J. *24*, 2464–2474.

Yin, Y.I., Bassit, B., Zhu, L., Yang, X., Wang, C., and Li, Y.M. (2007). {gamma}-Secretase Substrate Concentration Modulates the Abeta42/Abeta40 Ratio: IMPLICATIONS FOR ALZHEIMER DISEASE. J. Biol. Chem. *282*, 23639–23644.

Zhang, H., Ma, Q., Zhang, Y.W., and Xu, H. (2012). Proteolytic processing of Alzheimer's β-amyloid precursor protein. J. Neurochem. *120* (*Suppl 1*), 9–21.

Zhou, L., Brouwers, N., Benilova, I., Vandersteen, A., Mercken, M., Van Laere, K., Van Damme, P., Demedts, D., Van Leuven, F., Sleegers, K., et al. (2011). Amyloid precursor protein mutation E682K at the alternative β-secretase cleavage β′-site increases Aβ generation. EMBO Mol. Med. *3*, 291–302.